Journal of Proteomics 150 (2017) 242–251

Contents lists available at ScienceDirect

Journal of Proteomics

journal homepage: www.elsevier.com/locate/jprot

Antibacterial mechanism of daptomycin antibiotic against *Staphylococcus aureus* based on a quantitative bacterial proteome analysis

Wen Ma [a], Dan Zhang [a], Guoshun Li [a], Jingjing Liu [a], Gu He [a], Peng Zhang [b], Li Yang [a], Hongxia Zhu [c], Ningzhi Xu [a,c], Shufang Liang [a,*]

[a] State Key Laboratory of Biotherapy and Cancer Center, West China Hospital, Sichuan University/Collaborative Innovation Center for Biotherapy, Chengdu 610041, PR China
[b] Department of Urinary Surgery, West China Hospital, West China Medical School, Sichuan University, Chengdu 610041, PR China
[c] Laboratory of Cell and Molecular Biology, State Key Laboratory of Molecular Oncology, Cancer Institute & Cancer Hospital, Chinese Academy of Medical Sciences, Beijing 100034, PR China

ARTICLE INFO

Article history:
Received 23 November 2015
Received in revised form 6 September 2016
Accepted 26 September 2016
Available online 29 September 2016

Keywords:
Daptomycin
Staphylococcus aureus
Antibacterial activity
Quantitative proteomic

ABSTRACT

Daptomycin (DAP) is a novel lipopeptide antibiotic which exhibits excellent antibacterial activity against most clinically relevant Gram-positive bacteria, but the DAP-targeting protein molecules against host bacterial infection are far from clear. In order to discover bacterial protein response to DAP treatment, an iTRAQ-based quantitative proteomic analysis was applied to identify differential bacterial proteome profiling of *Staphylococcus aureus* (*S. aureus*) ATCC 25923 to 0.125 μg/ml DAP exposure. Totally 51 bacterial proteins were significantly changed with DAP treatment, among which 34 proteins were obviously up-regulated and 17 proteins were down-regulated. Meanwhile, 139 bacterial cell membrane (CM) proteins were identified, and 7 CM proteins were significantly altered to decrease CM potential to disrupt bacterial cell membrane. Especially the up-regulation of NDK and down-regulation of NT5 in several *S. aureus* strains are validated to be a universal variation tendency response to DAP treatment. Under DAP exposure, bacterial membrane potential is decreased and cell membrane is disrupted, and bacterial chromosome is aggregated, which contributes to bacterial DNA rapid release and induces bacteria death within 2–5 h. In general, multiple bacterial protein expressions are changed in response to DAP antibiotic exposure, which disrupts host bacterial physiology by multiple cellular levels. To our knowledge, this is the first time to exactly identify infectious bacterial proteins in response to DAP antibiotic action. Our findings help better understand DAP antibacterial mechanism and develop novel DAP derivatives against the upcoming antibiotic-resistant bacterial infection.

Biological significance: DAP is a novel lipopeptide antibiotic that it exhibits excellent in vitro activity against most clinically relevant Gram-positive bacteria, and the investigations on its pharmaceutical action mode of DAP have dramatically increased in the past decade due to its unique antimicrobial mechanism. However, the target molecules of DAP acting on the infectious bacteria, are far from clear. The state-of-the-art quantitative proteomic technologies provide new avenues to uncover underlying mechanism of antibiotics. Our research main aims to identify bacterial proteome profiling of host strain *S. aureus* response to DAP treatment through an iTRAQ-based quantitative proteomic analysis, which contributes to understand DAP efficient antibacterial activity and the microbial-antibiotic interactions.

1. Introduction

Daptomycin (DAP), commercially also called Cubicin made by Cubist Pharmaceuticals, originally is approved for the treatment of bacteremia and right-sided endocarditis caused by *Staphylococcus aureus* (*S. aureus*) and methicillin-resistant *S. aureus* (MRSA) in 2003 [1,2]. DAP is a novel lipopeptide antibiotic that displays rapid bactericidal activity in vitro against most clinically relevant Gram-positive (G^+) bacteria [1,2]. By now it exhibits excellent bactericidal activity against 6737 clinical G^+ strains, and the minimal inhibitory concentration (MIC) of which is ranged from 0.12 to 8 mg/l [3]. DAP also shows an activity against multidrug-resistant G^+ pathogens, including vancomycin-resistant *S. aureus* [4–7].

As a highly efficient antibacterial drug, the investigations on its pharmaceutical action mode of DAP have dramatically increased in the past decade. A widely accepted hypothesis of DAP antimicrobial activity is that it inhibits the lipoteichoic acid biosynthesis of G^+ pathogens to dissipate bacterial cell membrane across the cytoplasmic membrane [8,9]. Other studies indicate that DAP is a membrane-targeting antibiotic, which binds to Ca^{2+} to form a micellar structure in solution and

* Corresponding author at: State Key Laboratory of Biotherapy, West China Hospital, Sichuan University, No.17, 3rd Section of People's South Road, Chengdu 610041, PR China.
E-mail address: zizi2006@scu.edu.cn (S. Liang).

http://dx.doi.org/10.1016/j.jprot.2016.09.014

oligomerizes in cell membrane in the presence of 1 M equivalent of calcium ion [10]. And this oligomer contributes to delivering DAP to cell membrane of *S.aureus* [11,12], which results in the dissipation of cell membrane potential and potassium ion efflux, ultimately leads to cell death [8,13]. However, the target molecules of DAP acting on the infectious G^+ bacteria, are far from clear.

At present, the state-of-the-art proteomic technologies provide new avenues to uncover underlying mechanism of antibiotics [14]. Microbial proteomics has been developed greatly in revealing microbial pathogenicity, metabolism, biomarker discovery, and drug mechanism [15,16]. For example, proteins from various *S. aureus* strains were analyzed using one- or two-dimensional electrophoresis (2-DE) under different conditions, and the protein alterations in microorganism allow for understanding microbial cellular processes and particular functions [17–19]. More importantly, the development of chromatographic separations and MS–based quantitative proteomics, including the gel-free approach, LC-MS/MS, isobaric tagging reagent for quantitative proteomic analysis (iTRAQ) and the selected reaction monitoring, has contributed to identification of microbial pathogens [20] and bacterial proteins response to drug treatment [21].

In this study, our research aims to identify cellular proteome profiling of *S. aureus* response to the antibiotic DAP treatment through an iTRAQ-based quantitative proteomic approach, which enables us to further discover the functional characterization of the infectious bacterial proteins and the antibacterial molecular mechanism of DAP.

2. Materials and methods

2.1. Bacterial strains and growth conditions

The bacterial strains including *S. aureus* ATCC 25923, *S. aureus* CMCC 26003, *S. aureus* ATCC 6538 and methicillin sensitive *S. aureus* (MSSA), were stored as a 20% glycerol stock at −80 °C until used. Each strain was re-streaked from glycerol stocks to culture on Mueller-Hinton agar, then was inoculated into 5 ml of Mueller Hinton broth (MHB) to grow overnight at 37 °C with constant shaking.

For detection of bacterial growth response to the antibiotic treatment, it is necessary to add final concentration of 50 μg/ml Ca^{2+} and 10 μg/ml Mg^{2+} into MHB to exert DAP activity. Bacterial culture in Ca^{2+}, Mg^{2+} - containing MHB media was treated with different concentrations of DAP at 37 °C for 18 h with gentle shaking. And under the same conditions with no DAP exposure, the mock of bacterial culture was incubated with 1% DMSO as the negative control of antibiotic treatment.

2.2. Minimal inhibitory concentration of DAP

The antibacterial activity of DAP towards *S. aureus* was evaluated by the broth micro-dilution assay [22]. DAP was serially diluted two folds in culture in 96-well plates to obtain final concentrations ranged from 0.0625 to 1 μg/ml. An equal volume of 10 μl culture, approximately containing 5×10^5 cfu/ml *S. aureus*, was added to each well to incubate at 37 °C for 18 h, and the optical density at 600 nm (OD_{600nm}) was measured. The minimal inhibitory concentration (MIC) was determined as the lowest concentration which completely inhibited the bacterial growth. MIC was measured by three different experiment repeats.

2.3. Time-kill kinetic analysis

In order to determine an optimal DAP treatment concentration for the bacterial proteome identification, a time-kill kinetic analysis [18], was performed on *S. aureus* ATCC 25923. The bacteria were cultured in MHB media respectively with 0.25MIC, 0.35MIC, 0.5MIC, MIC, 2MIC of DAP exposure for 18 h, and each concentration of cultures was collected to detect OD_{600nm} for 3 times ($n = 3$). The DAP concentration, which exerts a 50–80% growth inhibition on bacteria at an exponential growth phase, would be determined as the drug usage quantity.

2.4. Protein extraction

S. aureus ATCC25923 cells at an exponential growth phase were cultured in MHB, containing 50 mg/l Ca^{2+} and 10 mg/l Mg^{2+} with 0.125 μg/ml DAP treatment. Bacterial cell pellets were collected by centrifugation at 10,000 ×*g* at 4 °C for 20 min. To extract cellular proteins, the harvested cells were washed twice with 0.9% (*w*/*v*) NaCl, and then 200 μl of 40 μg/ml lysostaphin (BBI, Markham, Canada) was added followed by incubation on ice for 10 min to remove cell walls. After centrifugation with 3000 ×*g* for 1 min at 4 °C, cell precipitation was resolved in 200 μl extraction buffer (50 Mm Tris-HCl, pH 8.0, 0.2 mM EDTA,100 mM NaCl, and 0.1% (v/v) Triton X-100). Proteins were extracted by sonication using a 950-Watt Ultrasonic processor (XINYI-IID) at 30% amplitude for 15 min on ice, with pulse durations of 3 s on and 9 s off. Then cellular debris was removed by centrifugation at 10,000 ×*g* for 30 min at 4 °C, and the supernatant was concentrated by precipitation with ice-cold acetone (1:6, v/v) at −20 °C for 4 h. Finally, protein concentration was determined using the protein assay kit (Bio-Rad, catalog No. 500-006) based on the Bradford method.

2.5. The iTRAQ labeling

A total of 120 μg of proteins per sample was used for each iTRAQ labeling. Protein samples were reduced, cysteine blocked, digested and labeled with respective isobaric tags using an iTRAQ® reagent Multiplex kit (PN 4352135, AB Sciex, CA, USA) according to manufacturer's protocols. To block cysteine residues, 20 μl dissolution buffer, 1 μl denaturant and 2 μl reducing reagent were respectively added to each of two sample tubes. The samples were incubated at 60 °C for 1 h, then 1 μl cysteine blocking reagent was added to incubate in the dark at room temperature for 10 min. For tryptic digestion, 10 μl of 1 μg/μl trypsin solution (Trypsin Gold, Promega, Madison) were used to treat each of samples overnight at 37 °C. The iTRAQ experiment was performed on two groups. One group was the DAP-treated bacterial proteins with 114 labeling, and another group without drug treatment was the experimental control with 116 labeling. The two samples were individually labeled with iTRAQ reagents 114,116 for 1 h at room temperature. The labeled peptides from two groups were then equally mixed and dried using a Speed Vac centrifuge (Thermo Electron Corporation, SPD131DDA, USA).

2.6. LC-MS/MS identification

Peptide mixtures from two groups of labeled peptides were separated by using Easy nanoLC (Thermo Scientific, San Jose, CA) and MS profiling spectra were obtained on a Q-Exactive mass spectrometer (Thermo Scientific, San Jose, CA). The iTRAQ-labeled peptides were loaded onto a trap column (2 cm × 100 μm, 5 μm, C18,Thermo scientific column), and separated using a reverse-phase column (75 μ m × 100 mm, 3 μm, C18, Thermo scientific) with a 220-min gradient at a flow rate of 250 nl/min. The mobile phase A was 0.1% formic acid in LC/MS-grade water, and the mobile phase B was 0.1% formic acid in 84% acetonitrile. The peptides were separated with a linear gradient 0–35% B in 200 min, 35%–100% B in 16 min, and 100% B in 4 min. Survey scans were acquired over a mass range of 300 to 1800 at resolution of 70,000. For MS/MS analysis, the top10 intense ions were selected for fragmentation by high energy collision dissociation (HCD) at normalized energy of 30%. The MS/MS scans were acquired at resolution of 17,500. The MS identification was performed in duplicate.

The collected raw data were processed using the Proteome Discoverer software (version1.3, Thermo Scientific). The Mascot search engine (v2.2, Matrix Sciences, London, UK) was utilized to search against the UniProt database, *Staphylococcus aureus* species which contains 478,846 sequences (version 3.35, Jan 14th, 2013). The parameters for

database searching were set as following: (i)the mass tolerance was set as 0.1 Da for MS/MS and 20 ppm for MS, (ii) trypsin enzyme specificity and two max-missed cleavages were allowed, (iii) the fixed modification included carbamidomethylation, iTRAQ8plex (N-term), iTRAQ8plex (K), Oxidation (M) and iTRAQ8 plex (Y). In case multiple peptides were identified for certain proteins, the peptide ratios were averaged to obtain protein ratios.

2.7. Real-time quantitative PCR

In order to detect the expression levels of genes, 1 mg of bacterial cell pellets obtained from 10 ml of culture was treated with 200 ml of 40 μg/ml lysostaphin for 5 min at 37 °C, and the sample was performed to extract total RNA with Trizol reagent (Life technology). The total RNA was resolved in nuclease-free water and stored at −80 °C for further use.

The reverse transcription reaction for cDNA (iScript cDNA synthesis kit, Bio-Rad) was performed in 20 μl of reaction mixture including 1 μg of total RNA as the templates, 4 μl of 5 × iScript reaction buffer and 1 μl of iScript reverse transcriptase. Real-time quantitative PCR (q-PCR) was performed using the SYBR Green Supermix kit (Bio-Rad) on a Bio-Rad CFX96 system according to the manufacturer' instructions. All primers for q-PCR were synthesized by Invitrogen Company in China. The PCR primers for nucleoside diphosphate kinase (NDK) were (F) 5′-AGAAAAGGACTAAAACTTGTCGGTG-3′ and (R) 5′-ACTGGTGCTGATG TAATAAATGAAA-3′. Primers for (5′-nucleotidase) NT5 were (F) 5′-GATAAGAGTAAAGAATCACGCAGACA-3′ and (R)5′-CTACCATACATTGG GTTAGGGAAAA-3′. Primers for triosephosphate isomerase (TPI) were (F) 5′-CGTTGTTATCGGTCATTCTG-3′and (R) 5′-TTTACCACTTTCACG CTCTT-3′.The 16s rRNA of *S. aureus* was taken as a control of comparison in q-PCR, and its primers were designed (F) 5′-TACACACCGCCCGT CACA-3′ and (R) 5′-CTTCGACGGCTAGCTCCTAAA-3′.

Each q-PCR reaction mixture (10 μl) was composed of 5 μl SYBR Green supermix, 0.4 μl forward primer, 0.4 μl reverse primer, 3.2 μl RNase-free water, and 1 μl of the cDNA template. The reaction condition was set as following procedures, including initial DNA denaturation for 3 min at 95 °C; 39 cycles of 30 s denaturation at 95 °C, 30 s annealing at 50 °C (for NDK), 59 °C (for NT5) or 55 °C (for TIP), then a final elongation at 72 °C for 10 min extension. Each gene expression was quantified by q-PCR in a strain for three times ($n = 3$).

2.8. Bacterial DNA quantification

In order to detect bacterial DNA from died bacteria releasing into the culture media, *S. aureus* was cultured in MHB with DAP exposure for 0.5 h, 1 h,2 h,3 h,5 h and 18 h respectively. Along with the bacterial death response to DAP treatment, the bacterial DNA released into the culture media, which was quantified with Quant-iT™ PicoGreen® dsDNA Assay Kit (Life Technologies, USA). 1.5×10^8 cfu/ml bacteria, including *S. aureus* ATCC 25923, *S. aureus* CMCC 26003, *S. aureus* ATCC 6538 and MSSA, were individually cultured in 5 ml of DAP-containing MHB, and the concentration of DAP was depended upon the MIC for each strain. Because the MIC of DAP against *S. aureus* ATCC 25923, ATCC 6538 and MSSA was 0.25 μg/ml for 5×10^5 cfu/ml bacterial cells, and totally 75 μg DAP was added to treat 1.5×10^8 cfu/ml bacteria to detect the bacterial DNA content. Similarly, the DAP usage for 1.5×10^8 cfu/ml *S.aureus* CMCC 26003 cells was determined as 18.75 μg.

The bacterial DNA in culture supernatant was collected by centrifugation at 10,000 × *g* for 3 min. 100 μl of the diluted bacterial DNA sample (a 10-fold dilution with TE buffer) was mixed with 100 μl Picogreen reagent (1:200 diluted solution), and the mixture was added to each well of a 96-well plate to incubate at room temperature for 5 min in dark. Then the fluorescence intensity at 480 nm excitation and 520 nm emission was detected to calculate DNA content with a Varioskan Flash spectral scan multimode plate reader (Thermo Fisher Scientific, USA).

2.9. Transmission electron microscopy analysis

In order to observe bacterial morphology and ultrastructure alteration under DAP treatment via a transmission electron microscopy (TEM) analysis, totally 9×10^9 *S. aureus* ATCC 25923 were cultured in 60 ml MHB overnight with or without 75 μg DAP treatment, and cells were harvested by centrifugation and washed with 0.1 M phosphate buffer saline (PBS) for three times. Cell pellets with 2.5% glutaraldehyde fixative were post-fixed in 1% osmium tetraoxide and incubated at room temperature for 1 h. After incubation, the sample was dehydrated with graded ethanol-PBS solutions as 20% ethanol for 10 min, 40% ethanol for 10 min, 60% ethanol for 10 min, 80% ethanol for 15 min, 90% ethanol for 15 min, and twice in 100% ethanol for 20 min. The samples were fixed in epoxy resin and left to polymerize for 2 days. Each sample was cut into approximately 90-nm thin slices, and lead citrate on grids. Morphological and ultrastructural alterations of the bacteria were observed and photographed by a TEM analysis with a field-emission gun operating at 200 kV (Tecnai G^2 F20, FEI Company, USA).

2.10. Fluorimeter assay for bacterial membrane potential

Bacterial membrane potential of *S. aureus*, response to DAP exposure, was measured by using a fluorescent assay. *S. aureus* cells were cultured with 0.5MIC of DAP treatment. 200 μl of *S. aureus* cell samples was transferred into a 96-well plate, and a membrane potential sensitive dye, 50 μM $DiSC_3$ (3,3′-dipropylthiadicarbocyanine iodide; Life technology), was added into each well to incubate for an additional 5 min at 37 °C. The fluorescence intensity was detected on a Varioskan Flash spectral scan multimode plate reader (Thermo Fisher Scientific, USA), with an excitation wavelength of 622 nm and the fluorescence emission at 670 nm.

3. Results

3.1. Bacterial growth with DAP exposure

Firstly, the MIC of DAP against *S. aureus* was obtained. The MIC of DAP towards *S. aureus* ATCC 25923 was 0.25 μg/ml. And the MIC against other strains, including *S. aureus* CMCC 26003, *S. aureus* ATCC 6538 and MSSA, was respectively 0.0625 μg/ml, 0.25 μg/ml and 0.25 μg/ml in turn.

Furthermore, the growth profiling of *S. aureus* ATCC 25923 response to different concentration of DAP treatment was analyzed. In MHB medium inoculated with 5×10^5 cfu/ml of *S. aureus* ATCC 25923, the bacterial growth curves documented the inhibitory effect of DAP on this strain. Bacterial growth was completely inhibited under either 0.25 μg/ml (MIC) or 0.5 μg/ml (2MIC) of DAP exposure for 2–18 h (Fig. 1). And the bacteria growth was relatively inhibited by 60%

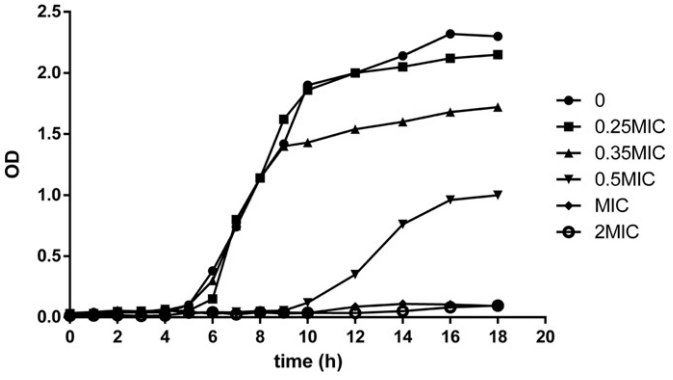

Fig. 1. Growth curves of *S. aureus* ATCC 25923 against DAP treatment. Bacterial growth is inhibited under MIC or 2MIC of DAP exposure for 2–18 h. While the bacterial growth, under 0.25 MIC of DAP treatment, was similar with the normal culture. Each point represented OD of bacteria measured by three different experiment repeats.

under 0.5 MIC of DAP treatment. While the bacteria growth was no significant difference between 0.25 MIC of DAP treatment and the control samples. According to the time-kill kinetics on *S. aureus* ATCC 25923, 0.125 μg/ml, a half of MIC of DAP against this strain, was determined as a sub-inhibitory concentration for analyzing bacterial proteome profiling response to DAP treatment.

3.2. MS data analysis

The iTRAQ-based quantitative proteomic strategy, a relative and absolute protein quantification for multiple samples simultaneously [23], was applied to analyze differential proteome expression of *S. aureus* ATCC 25923 response to DAP treatment. This iTRAQ labeling method of tracking relative concentrations of different proteins was used and summarized in our previous reports [24,25]. The differential expression levels (ratios) of proteins in DAP-treated bacteria versus the untreated control were calculated based on the peak intensity iTRAQ-labelings in MS/MS scans.

Overall, 872 proteins were confidently identified at 1% or less false discovery rate (FDR) among which 789 proteins derived from 4566 peptides were quantified. The iTRAQ ratios (treated/untreated) of 789 proteins nearly exhibited a normal distribution (Fig. 2A). The error factor (EF) and 95% confidence interval (95% CI) and standard deviation (SD) values were calculated based on peak ratios obtained from all identified peptides. The average SD value was 0.30 for all 789 quantified proteins, therefore a significantly changed protein was defined when the changed ratio has at least five times of the average SD ($\overline{SD}$). A differential (changed) protein was simultaneously met the conditions of EF < 2, change ratio > 5-fold of $\overline{SD}$ and student *t*-test at *p*-value < 0.05. More specially, the differential proteins were included into the upregulated proteins with expression level over 1.86-fold increase, and the down-regulated ones with expression below 0.57-fold decrease. According to these quantitative criteria, 51 proteins were found to have significant expression changes between the DAP-treated and the control group (Table 1). Among these altered proteins, 34 proteins were increased with ranging from 1.86 to 9.85-fold, and three of them have significantly high expression (>4.0-fold) after DAP treatment, whereas 17 proteins were decreased with ranging from 1.77 to 3.68-fold.

3.3. Molecular functions of the altered proteins

The differentially expressed proteins were divided into several groups based on the Gene Ontology (GO) molecular function analysis (Table 1). For example, 23 proteins (45%) participate in catalytic activity, and 9 proteins (18%) exhibit nucleotide binding activity. Three (6%) proteins have a role in protein binding (including cofactor binding and repressor protein), two proteins (4%) are considered to have transporting function and one protein is related to toxin. In addition, 13 proteins (25%) were annotated as unknown functions (Fig. 2C).

The subcellular localization of the 51 changed proteins were also categorized (Fig. 2D). Among them, 7 proteins locate in cell membrane, 19 proteins locate in cytoplasm (including one ribosomal protein) and two proteins are mainly distributed in extracellular. The other 23 proteins are unclear with exactly cellular localization.

3.4. Expression profiling of cell membrane proteins

Of all 789 quantified bacterial proteins, in total 139 cellular membrane proteins were identified, and 7 of them were significantly altered. These 7 cell membrane (CM) proteins were classified into 2 groups according to their contributions to the relative negative charge in membrane surface (Table 2), which would be beneficial to DAP binding and the antibacterial action. Except to 2 increased proteins (succinate dehydrogenase cytochrome *b*-556 subunit and ATP synthase subunit A) with a positive charge (pI > 7), the 5 proteins (nucleoside diphosphate kinase

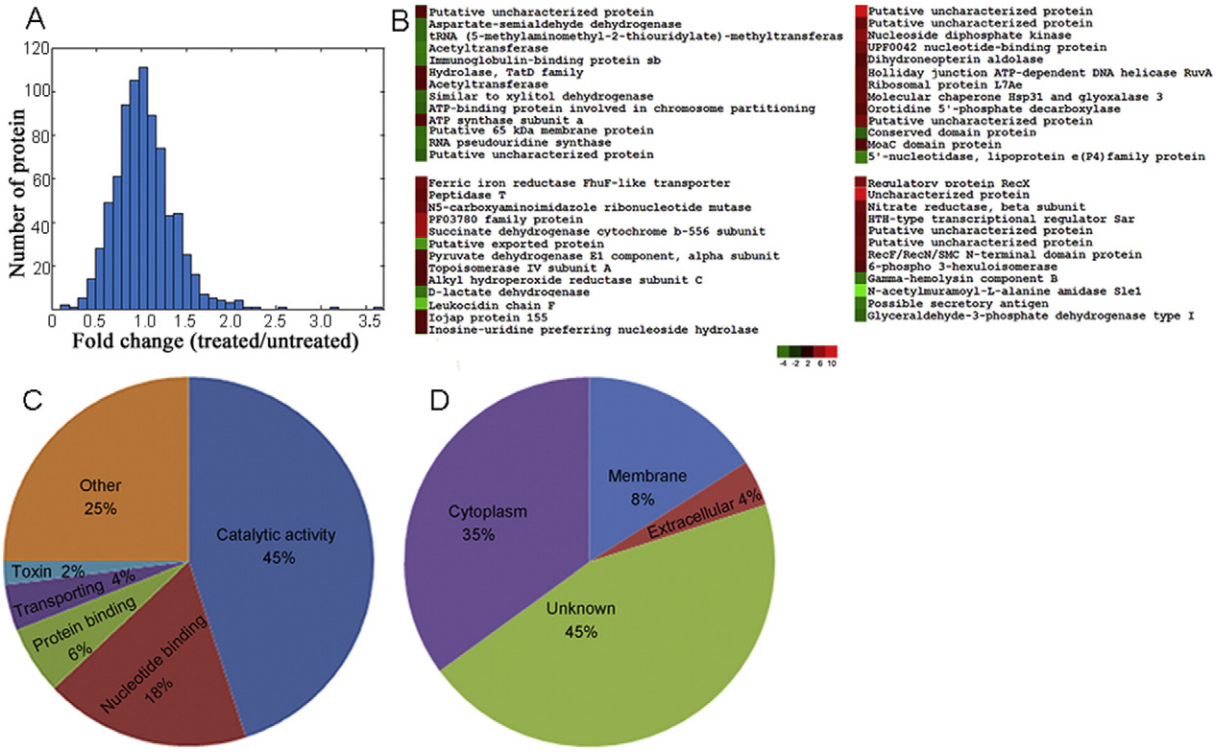

Fig. 2. Proteome profiling identified in *S. aureus* ATCC 25923 with DAP exposure. (A) The peak intensity ratios of m/z = 114 versus m/z = 116 (treated vs. untreated) from 789 quantitative identified proteins exhibited a normal Gausses distribution. (B) Fifty-one bacterial proteins significantly altered, including 17 proteins down-regulated (green panes) and 34 up-regulated over 1.86-fold (red panes). (C) 51 differentially expressed proteins were functionally sorted into 6 functional categories according to the gene ontology annotation. (D) Cellular localization of the 51 altered proteins.

Table 1
Cluster analysis of the altered proteins.

Molecular function	Accession number	Protein name	Fold change[a]	pI[b]	MW [kDa]	Localization[c]
Catalytic activity(23)	295127992	Succinate dehydrogenase cytochrome *b*-556 subunit	3.25 ± 0.22↑	8.72	20.08	Membrane
	282319755	AIR carboxylase	2.35 ± 0.11↑	5.94	17.06	
	283471618	Nitrate reductase beta subunit	2.43 ± 0.37↑	5.44	55.27	
	298695541	Inosine-uridine preferring nucleoside hydrolase	1.92 ± 0.22↑	5.21	32.66	Cytoplasm
	282320444	5′-nucleotidase	2.24 ± 0.07↓	9.49	33.34	
	298695140	Regulatory protein RecX	2.67 ± 0.05↑	5.85	29.05	
	257846453	Peptidase T	2.19 ± 0.01↑	4.88	45.92	
	150373525	Molecular chaperone Hsp31 and glyoxalase 3	2.31 ± 0.19↑	5.05	32.16	
	375034342	tRNA (5-methylaminomethyl-2-thiouridylate)-methyltransferase	1.94 ± 0.47↓	5.82	36.55	
	253724222	Aspartate-semialdehyde dehydrogenase	1.93 ± 0.61↓	5.08	36.26	
	257273054	D-lactate dehydrogenase	2.06 ± 0.16↓	5.48	24.91	
	156721660	Orotidine 5′-phosphate decarboxylase	2.04 ± 0.01↑	6.28	25.60	
	383357693	Pyruvate dehydrogenase E1 component alpha subunit	2.00 ± 0.41↑	4.88	41.30	
	282320324	Dihydroneopterin aldolase	1.97 ± 0.33↑	5.82	13.74	
	377697984	Alkyl hydroperoxide reductase subunit C	1.86 ± 0.27↑	5.14	9.78	
	257847305	Acetyltransferase(S.aureus A9635)	1.87 ± 0.76↑	4.67	19.88	
	257279654	Acetyltransferase(S.aureus 68–397)	2.19 ± 0.14↓	5.16	19.95	
	365237094	*N*-acetylmuramoyl-L-alanine amidase Sle1	3.68 ± 0.69↓	9.63	32.5	Extracellular
	282331375	Glyceraldehyde-3-phosphate dehydrogenase type I	1.87 ± 0.64↓	6.05	36.98	Unknown
	253726636	Putative uncharacterized protein	1.77 ± 0.30↓	10.05	10.29	
	257275550	6-phospho 3-hexuloisomerase	2.01 ± 0.37↑	5.49	19.60	
	375018476	Hydrolase	1.89 ± 0.12↑	5.33	28.86	
	282329413	ATP-binding protein involved in chromosome partitioning	1.77 ± 0.12↓	5.31	38.38	
Nucleotide binding(9)	365164976	Nucleoside diphosphate kinase	2.69 ± 0.17↑	5.53	16.55	Membrane
	257278840	Topoisomerase IV subunit A	1.86 ± 0.15↑	6.42	90.99	
	344176905	HTH-type transcriptional regulator Sar	2.22 ± 0.10↑	8.53	14.15	Cytoplasm
	156722095	Holliday junction ATP-dependent DNA helicase RuvA	2.29 ± 0.51↑	6.23	22.27	
	408428732	Similar to xylitol dehydrogenase	1.87 ± 0.22↓	5.16	34.34	
	365245635	RNA pseudouridine synthase	2.02 ± 0.09↓	7.64	21.59	
	253728322	DNA-dependent DNA polymerase family X	9.85 ± 0.78↑	4.70	10.43	Unknown
	377739719	Putative uncharacterized protein	2.57 ± 0.38↑	5.88	10.54	
	7328270	hypothetical protein	2.54 ± 0.29↑	5.96	31.04	
Protein binding (3)	365243005	Ribosomal protein L7Ae	2.25 ± 0.31↑	10.08	7.72	Cytoplasm; ribosome
	282331292	Ribosomal silencing factor RsfS	1.92 ± 0.39↑	4.79	13.44	Unknown
	377749114	Immunoglobulin-binding protein sbi	2.11 ± 0.47↓	9.32	49.2	
Transporting (2)	377741740	ATP synthase subunit A	1.90 ± 0.32↑	9.33	24.75	Membrane
	375015204	Ferric iron reductase FhuF-like transporter	2.47 ± 0.34↑	6.54	27.25	
Toxin(1)	377709301	Gamma-hemolysin component B	2.06 ± 0.21↓	8.29	25.9	Extracellular
Others(13)	374363031	hypothetical protein SAVC_04870	4.86 ± 0.55↑	6.78	9.64	Unknown
	320143212	Putative uncharacterized protein	6.70 ± 0.33↑	5.01	6.63	
	371976235	PF03780 family protein	3.19 ± 0.27↑	7.43	13.26	
	383359444	RecF/RecN/SMC N-terminal domain protein	2.27 ± 0.56↑	5.38	47.05	
	365173901	Putative uncharacterized protein	2.20 ± 0.12↑	3.75	7.97	
	365164517	MoaC domain protein	1.97 ± 0.10↑	4.78	9.02	
	160367735	Putative uncharacterized protein	1.94 ± 0.15↑	4.67	23.75	
	334275314	Putative uncharacterized protein	2.34 ± 0.09↑	4.49	8.33	
	365225215	Putative 65 kDa membrane protein	1.95 ± 0.23↓	9.86	41.97	
	374396522	Putative uncharacterized protein	2.33 ± 0.53↑	4.56	9.73	
	377743258	Putative exported protein	2.56 ± 0.46↓	6.62	5.67	
	253726412	Possible secretory antigen	2.09 ± 0.27↓	9.54	12.75	
	334271011	Conserved domain protein	1.79 ± 0.38↓	7.24	8.01	

Notes: All quantitative data were recorded as mean ± SD (n = 2).
[a] The fold changes of differential proteins were calculated from 114/116 ratios, which should meet all parameters including p-value, fold-change and peak ratios.
[b] The isoelectric point of protein.
[c] The localization of proteins.

Table 2
Bacterial membrane proteins were altered with DAP treatment.

Charge[a]	Accession number	Protein name	Change ratio	pI[b]
Negative(−)	365164976	Nucleoside diphosphate kinase (NDK)	2.69 ± 0.17↑	5.53
	282319755	AIR carboxylase	2.35 ± 0.11↑	5.94
	283471618	Nitrate reductase beta subunit	2.43 ± 0.37↑	5.44
	375015204	Ferric iron reductase FhuF-like transporter	2.47 ± 0.34↑	6.54
	257278840	Topoisomerase IV subunit A	1.86 ± 0.15↑	6.42
Positive(+)	295127992	Succinate dehydrogenase cytochrome *b*-556 subunit	3.25 ± 0.22↑	8.72
	377741740	ATP synthase subunit A	1.90 ± 0.32↑	9.33

The experiment was performed in duplicate (n = 3).
[a] Protein shown a negative charge when the pI < 7 in neutral pH solution, while shown a positive charge when the pI > 7.
[b] The isoelectric point of protein.

(NDK), topoisomerase IV subunit A, AIR carboxylase, nitrate reductase beta subunit, ferric iron reductase FhuF-like transporter and topoisomerase IV subunit A) show negative charges (pI < 7) responsive to DAP treatment, which helps to form relatively negative surface charges. Regarding biological functions of 7 CM proteins, the up-regulated protein NDK is a major enzyme in nucleoside triphosphate synthesis [26,27]. Other four proteins, succinate dehydrogenase cytochrome *b*-556 subunit, AIR carboxylase, nitrate reductase beta subunit and ATP synthase subunit A participate in enzyme catalytic activity. Topoisomerase IV subunit A is concerned with nucleotide binding. The expression levels of CM proteins have influences on bacterial cell surface charges, which induces DAP to disturb membrane integrity and further disrupts nucleotide acid metabolism. Our proteome data supports previous hypothesis on a membrane-based mode of DAP action [28].

3.5. Expression change of NDK and NT5 with DAP exposure

We noticed that NDK and NT5 are two important enzymes for cellular nucleotide acid metabolism. The up-regulated protein NDK is a major enzyme in nucleoside triphosphate synthesis [26,27], and the decreased protein NT5 is a bacterial enzyme which specifically hydrolyzes 5′-nucleotides to release phosphoric acid [29,30]. Therefore the expression change of NDK and NT5 with DAP exposure was further validated in more different *S. aureus* strains.

Based on the isotope peak ratio of tag 114 versus tag 116 in MS, the protein NDK was averagely increased by 2.95 folds under DAP exposure. One representative peptide (LMQVPMELAETHYGEHQGK) of NDK was taken to quantify its expression level (Fig. 3A). The peak intensity ratio of isotope labeled peptides with iTRAQ tag 114 versus 116 was 3.50, which showed that the expression level of NDK was increased by 3.50-fold with the drug treatment. Similarly, NT5 was quantified to 2.24-fold down-regulation averagely from the two isotope peptide ratios (Table 3). For example, a peptide (SSAEVQQTQQASIPASQK) of NT5 with isotope peak ratio (m/z 114 versus 116) was 0.39 (34counts/78counts), which indicated that the NT5 expression was decreased by 2.56-fold by drug exposure (Fig. 3B). Meanwhile, the TPI, one housekeeping gene in *Staphylococci* [31], was no change (average change ratio was 1.00 ± 0.21) with drug treatment, which was taken as a comparison control for MS quantification. And an isotope peak intensity ratio of m/z114 versus m/z 116 from a peptide AVAGLSEDQLK of TPI were exampled to show almost identical (100counts/92counts = 1.09) in MS (Fig. 3C).

In order to detect the gene expression level of NDK and NT5 for DAP exposure, several *S. aureus* strains including *S. aureus* ATCC 25923, *S. aureus* CMCC 26003, *S. aureus* ATCC 6538 and MSSA were further validated to gene expression by q-PCR. Under the condition of 0.5MIC of DAP treatment, the gene expression of NDK in these strains was respectively increased by 2.75, 2.20, 3.17 and 1.91 fold ($p < 0.05$) (Fig. 4A), while NT5 gene was significantly decreased by 2.43, 2.02, 4.28 and 1.94 fold in turn

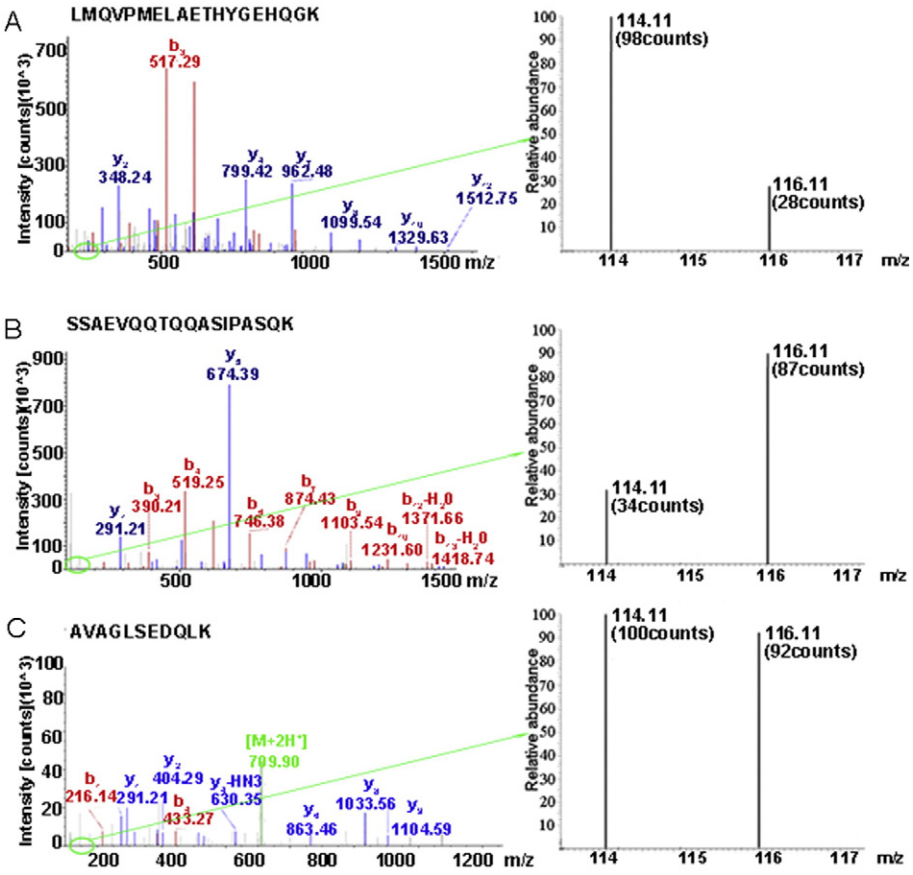

Fig. 3. Representative MS/MS spectra of NDK and NT5 to quantify protein expression levels. The control sample was labeling with iTRAQ reagent 116, and the DAP–treated sample was tagged with iTRAQ reagent 114. (A) The MS/MS spectra of one peptide with m/z 2198.49 of NDK were shown. The y-ion series in the MS/MS spectra readily assign the amino acid sequence as LMQVPMELAETHYGEHQGK. The local zoom spectra was shown and the peak intensity ratio of m/z114.11 versus m/z 116.11 (98/28 = 3.50), from an isotope labeling peptide LMQVPMELAETHYGEHQGK of NDK, shown NDK was up-regulated. (B) The MS/MS spectra of one peptide with m/z 1888.01 of NT5 were shown. The b-ion series in the MS/MS spectra readily assign the amino acid sequence as SSAEVQQTQQASIPASQK. The local zoom spectra was shown and the peak intensity of m/z114.11 was lower than m/z 116.11 (34/87 = 0.39). (C) The MS/MS spectra of one peptide with m/z 1130.25 of TPI were shown. The y-ion series in the MS/MS spectra readily assign the amino acid sequence as AVAGLSEDQLK. The local zoom spectra was shown and the peak intensity ratio of m/z114.11 versus m/z 116.11 (100/92 = 1.09), from an isotope labeling peptide AVAGLSEDQLK of TPI, were almost identical in MS.

Table 3
The isotope peptides of NDK and NT5 were identified by iTRAQ (n = 2).

Protein name	Peptide sequence[a]	Ion score[b]	Peptide ratio (114/116)[c]	Average protein ratio (114/116)[d]	Protein change-fold[e]
NDK	LMQVPMELAETHYGEHQGK	66.84	3.50	2.69 ± 0.17↑	2.95 ± 0.15↑
	NIIHGSDSLK	16.96	1.88		
NT5	SSAEVQQTQQASIPASQK	81.51	0.390	0.445 ± 0.07	2.24 ± 0.33↓
	ALYLQGYNSAK	49.01	0.553		
	QQGIPQAK	36.11	0.470		
	AkPVYGAK	19.43	0.422		
TPI	QTIADLSSK	42.24	0.94	1.003 ± 0.192	1.00 ± 0.21
	ANDVVGEQVK	33.15	1.18		
	AVAGLSEDQLK	20.91	0.76		
	APIIAGNWK	34.11	1.13		

[a] Unique peptides with iTRAQ tag labeling used for MS quantification.
[b] Probability-based Mascot scores.
[c] The peak intensity ratio was the DAP-treated sample with tag 114 versus the control with tag116 (114/116).
[d] The average peak ratio (114/116) of a protein. At least one peptide was used for quantification, and it was averaged when several peptides were used to quantify a protein.
[e] The change-fold of a protein, calculated from 114/116 ratio or its reciprocal (n = 2).

($p < 0.05$) (Fig. 4B). These results were completely consistent with the MS quantification in protein level. Therefore, the up-regulation of NDK and down-regulation of NT5 in *S. aureus* strains are a universal variation tendency response to DAP treatment.

3.6. DAP reduces cell membrane potential

Due to CM proteins with different charges, we evaluated DAP effects on cell membrane depolarization and potential loss in four *S. aureus* strains under conditions of at one-half the DAP MIC, which was used as the sub-inhibitory concentration for our proteomic analysis. The fluorescence of membrane potential-sensitive fluorescent probe $DiSC_3$ will decrease due to fluorescence dequenching when the dye partitions to the surface of polarized cells and the membrane potential is disrupted. Thereby, the depolarized cells produce higher signal than the control [32]. As shown in Fig. 5, cell fluorescence intensities were greatly increased for each stain when a half of MIC was respectively treated to *S. aureus* ATCC 25923, *S. aureus* ATCC 6538, MSSA (0.125 μg/ml DAP) and *S. aureus* CMCC 26003 (0.03125 μg/ml DAP) for 5 h ($p < 0.01$), which demonstrated bacterial membrane potential was greatly dissipated and membrane depolarization was caused. The biological effects on bacterial membrane potential are partly responsible for DAP antimicrobial activity [33].

3.7. DAP induces bacterial DNA rapid release

Furthermore, bacterial cell membrane morphology changes responsive to DAP treatment were observed by TEM. Bacterial cell membrane morphology and cell ultrastructure of *S. aureus* ATCC 25923 under 1 MIC of DAP (0.25 μg/ml) exposure overnight were both obviously different from the mock strain with no drug treatment (Fig. 6). Compared with the untreated strain (Fig. 6B, D), bacterial CM was disrupted and damaged with no membrane integrity (Fig. 6A), as well as the antibiotic caused bacterial chromosome aggregation (Fig. 6C), which were typical features that DAP exhibited antimicrobial effects on *S. aureus* to induce a quick release of bacterial DNA into cultured media (Fig. 7A).

According to the biological effects of DAP on bacterial cell membrane potential and nucleotide metabolism, we further quantitatively detected the amount of bacterial DNA release after DAP treatment. For *S. aureus* ATCC 25923, CMCC 26003, ATCC 6538 and MSSA, a quickly sudden release of bacterial DNA at a different time-point for DAP treatment 1–3 h, demonstrated that DAP has approached its maximum antibacterial activity for each strain (Fig. 7). For example, the amount of bacterial DNA release by DAP treatment for 3 h, 64.9 ng/ml, was 7.5-time higher than that for 2 h, 8.6 ng/ml in *S. aureus* ATCC 25923 (Fig. 7A). The released DNA for *S. aureus* CMCC 26003 was increased by 3.7-fold, from 41.8 ng/ml at DAP exposure time point 0.5 h to 156.9 ng/ml at drug treatment time point 1 h (Fig. 7B), and 21.2 ng/ml bacterial DNA at treat time point 0.5 h, was greatly increased to 4.7-fold, containing 99.7 ng/ml at drug treatment time point 1 h for *S. aureus* ATCC 6538 (Fig. 7D). However, a relatively gradual release of bacterial DNA was observed in MSSA (Fig. 7C), the amount of DNA release was significantly increased upon DAP treatment within 5 h, from14.9, 31.4, 42.8, 105.1 to 132.3 ng/ml at time point 0.5 h, 1 h, 2 h, 3 h and 5 h.

Generally DAP quickly promotes bacterial DNA release and leads to bacteria death within 2-5 h. For *S. aureus* ATCC 25923 and MSSA, the amount of bacterial DNA in culture supernatant was 81.2 ng/ml and 132.3 ng/ml respectively after DAP treatment for 5 h, which was almost

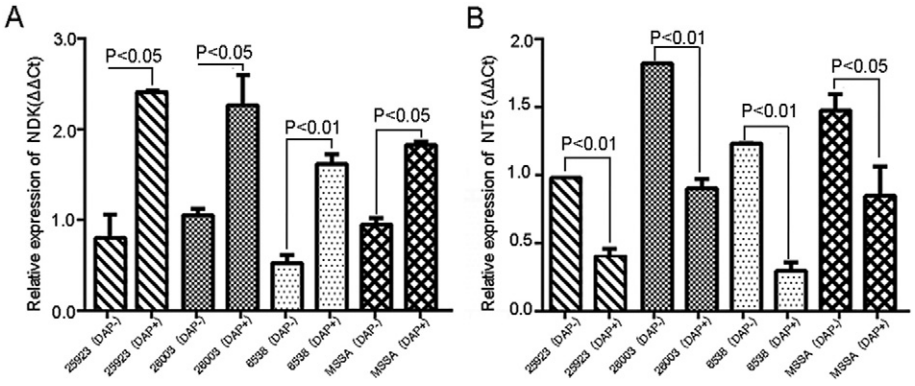

Fig. 4. Expression levels of NDK and NT5 in different *S. aureus* strains with DAP exposure. *S. aureus* ATCC 25923, CMCC 26003, ATCC 6538 and MSSA were selected to determine the expression level of NDK and NT5 under 0.5MIC of DAP exposure. Each gene expression was quantified by q-PCR in a strain for three times ($n = 3$). (A) The expression of NDK was increased by 2.75, 2.20, 3.17 and 1.91 fold on average ($p < 0.05$) in *S. aureus* ATCC 25923, CMCC 26003, ATCC 6538 and MSSA respectively. (B) The expression of NT5 gene was decreased by 2.43, 2.02, 4.28 and 1.94 fold ($p < 0.05$) respectively.

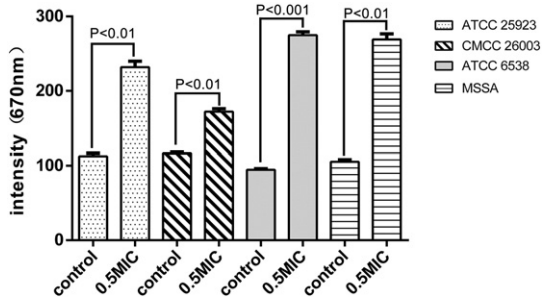

Fig. 5. DAP reduces bacterial membrane potential measured by fluorimetry assay (n = 3). *S. aureus cultures, including S. aureus* ATCC 25923, CMCC 26003, ATCC 6538 and MSSA, were incubated with or without a one-half MIC of DAP for 5 h to detect membrane potential respectively with 3 times (n = 3). The increase of fluorescence intensity means reductions of bacterial membrane potential.

equal with that with DAP exposure for 18 h (83.9 ng/ml and 136.2 ng/ml). At the drug action for 2 h, the amount of released DNA from *S. aureus* CMCC 26003 and ATCC 6538, 185.5 ng/ml and 152.4 ng/ml in turn, was similar with 191.3 ng/ml and 154.3 ng/ml after DAP treatment for 5 h, and this indicated the two *S. aureus* strains were almost killed after 2 h of antibiotic action.

4. Discussion

The proteomics tool enlarges our understanding for microbial behaviors upon different stimuli or environmental conditions. Although previous studies show the mode of action of DAP is different from any other known antibiotics, its exact antibacterial mechanism remains to be determined. Our proteomic data indicated that DAP at a half concentration of MIC would affect the expression levels of many functional bacterial proteins of host strain *S. aureus* ATCC25923, including some CM proteins. Especially these altered CM proteins confer upon their contributions for DAP binding directly or indirectly with bacterial membrane to exert antibacterial activity due to the enrichment of negative charge in bacterial CM surface. To our best knowledge, the present proteomic study is the first report to reveal the global changes of pathogenic bacteria proteins with DAP treatment, which helps us understand its acting molecules and develop novel DAP derivatives against conventional antibiotic-resistant bacterial infection. Of course current proteomic strategy has been widely applied for different microbial or antimicrobial proteome profiling. For example, a bacteriocin (nisin) in food poisoning has been identified to affect bacterial proteins associated to oxidative stress by a comparative proteomic study [34].

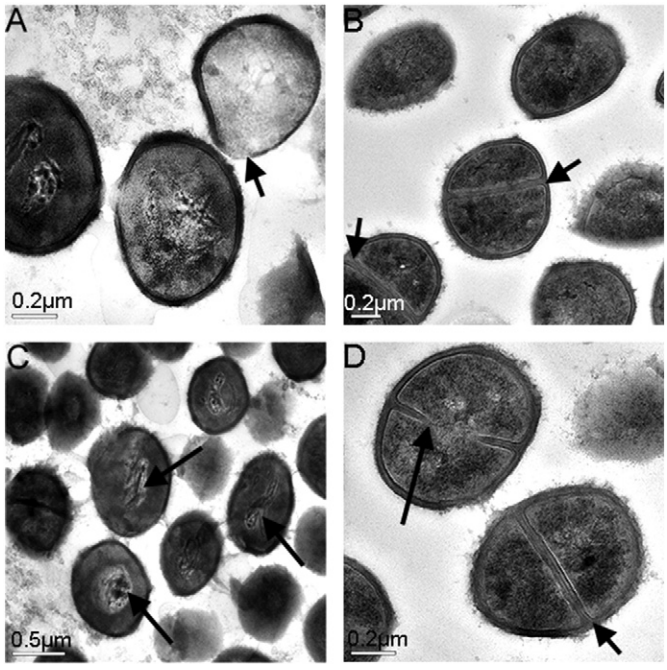

Fig. 6. Bacterial cell membrane and cell ultrastructure are obviously changed with DAP treatment. The *S. aureus* ATCC 25923 bacteria were incubated overnight with a MIC of DAP treatment (A, C) and no drug usage (B, D). (A) The damaged cell membrane was shown in arrows. (C) The clumps or aggregation of bacterial chromosome were indicated in arrows. While regular cell ultrastructures were visible with no antibiotic treatment on *S. aureus* ATCC 25923 cells (B, D). Scale bar represented 0.5 μm (A) and 0.2 μm (B, C, D), respectively.

Moreover, two significantly altered proteins, NDK and NT5, were noticed their functional roles in bacterial nucleotide acid metabolism. Structurally, NDK was negative in charge (pI < 7) with 2.95-fold upregulation while NT5 was positively charged (pI > 7) with 2.24-fold downregulation. Functionally, both of the two molecules were important enzymes correlated with purine metabolism. Based on the data set, we have demonstrated that the cooperative effects of DAP on CM damage and DNA release in *S. aureus* (Figs. 6 and 7). Therefore DAP not only acts on bacterial CM proteins to result in the decrease of membrane potential and depolarization, it but also affects bacterial DNA metabolism, accompanied with bacterial DNA efflux, to exert antibacterial activity. This double antibacterial pathways confer DAP with a broad spectrum and excellent bactericidal activity for serious bacterial infections even caused by MRSA and vancomycin-resistant *S. aureus*.

S. aureus is a human pathogen causing a wide variety of diseases ranging from wound infection to endocarditis, osteomyelitis, and sepsis [35]. Due to its ubiquity and its ability to survive in the terrestrial environment, it remains a major threat to human health in the hospitals and also in the community. *S. aureus* has become increasingly problematic in the past decades. Although DAP is a novel cyclic lipopeptide antibiotic displays rapid bactericidal activity against *S. aureus*, recently DAP-resistant pathogen is an increasing challenge in treating infections. Some clinical cases of DAP-resistance or the decreased susceptibility to DAP have been reported [36,37]. Some genetic changes may correlate with reduced susceptibility of DAP [38]. So far, this study has discovered the effects of DAP on *S. aureus* proteins by proteomics analysis, which greatly helps to completely understand microbial-antibiotic interactions and DAP antibacterial target proteins, as well as develop more efficient DAP-based derivatives with an altered pharmaceutical spectrum to address upcoming antibiotic-resistant pathogens.

Our quantitative proteomic analysis revealed 51 bacterial proteins, 34 up-regulated and 17 down-regulated, were significantly changed responsive to DAP exposure at sub-inhibitory concentration. The differentially expressed bacterial proteins involve in multiple biological functions including catalytic activity, nucleotide binding, protein binding and other biological activities. On the other hand, totally 139 identified strain proteins locate in bacterial cell membrane, 7 CM proteins were significantly altered in expression level which reduced bacterial membrane potential to help DAP disrupt bacterial CM to perform antibacterial activity. Moreover, the morphological and ultrastructural alterations of DAP-treated *S. aureus* ATCC 25923 via TEM observations clearly demonstrated bacterial cell membrane was disrupted and damaged with no membrane integrity, and bacterial chromosome was aggregated, which resulted in bacterial DNA rapid release and induced bacteria death quickly.

Especially two important bacterial nucleotide acid metabolism associated proteins [26–29], the up-regulation of NDK (nucleoside-diphosphate kinase) based on GenPept accession no. WP_000442484 and down-regulation of NT5(5′-nucleotidase) based on GenPept accession no.WP_001033881 are validated to be a universal variation tendency responsive to DAP treatment in several *S. aureus* strains. NDK and NT5 both take part in purine metabolism in other reports, including deoxyguanosine (Fig. 3A in Ref. [39]) and deoxyadenosine synthesis (Fig. 3B in Ref. [39]). The NDK is located on CM and it exhibits a major role in the synthesis of nucleoside triphosphates (NTPs) or the deoxy

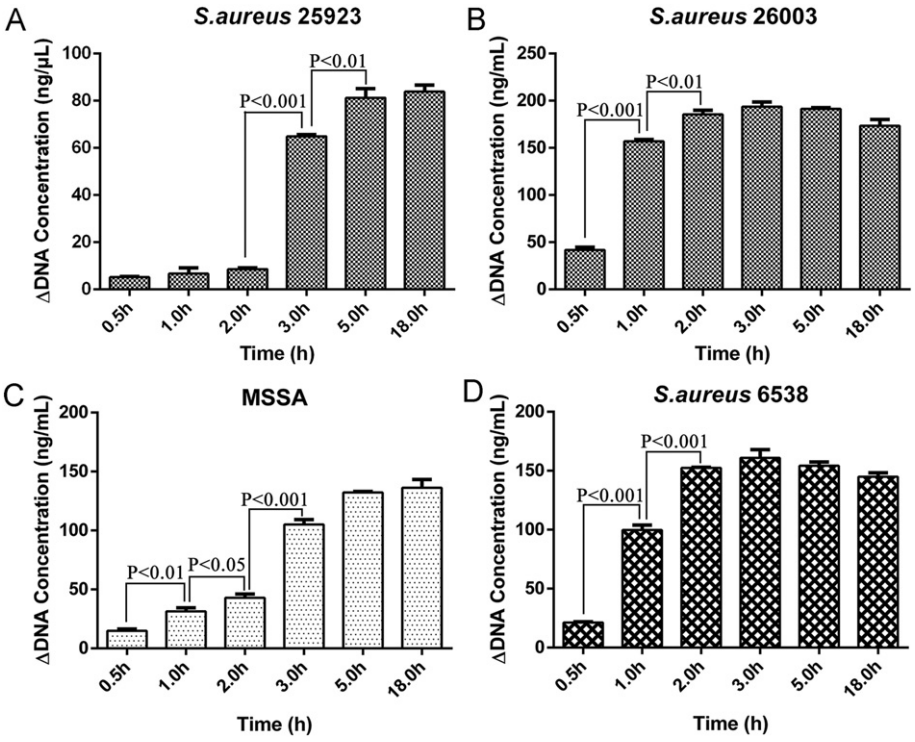

Fig. 7. DAP rapidly induces bacterial DNA release. 7.5×10^8 bacterial cells respectively from *S. aureus* ATCC 25923, CMCC 26003, MSSA and ATCC 6538 were treated with 1 MIC of DAP treatment for overnights (n = 3). (A) The amount of DNA release from treated *S. aureus* ATCC 25923 was 5.2, 6.6, 8.6, 64.9, 81.2 and 83.9 ng/ml at the time point of 0.5, 1, 2, 3, 5 and 18 h. Similarly, the released DNA from *S. aureus* CMCC 26003 was 41.8, 156.9, 185.5, 193.6, 191.3 and 173.5 ng/ml in turn under drug treatment for 0.5, 1, 2, 3, 5 and 18 h (B). And at the same conditions, DNA release from treated MSSA strain was 14.9, 31.4, 42.8, 105.1, 132.3, 136.2 ng/ml (C), while there was 21.2, 99.7, 152.4, 60.9, 154.3, 144.9 ng/ml DNA detected from *S. aureus* ATCC 6538 (D).

derivatives, which play important roles in bacterial growth, signal transduction and pathogenicity [27]. The ATP gamma phosphate is transferred to the NDP beta phosphate via a ping-pong mechanism [40], using a phosphorylated active-site intermediate. Meanwhile, NT5 is associated with the adenosine synthesis in *S. aureus* [26,41]. NT5 is a hydrolase acting on ester bonds, it is a bacterial membrane-bound enzyme which specifically hydrolyzes 5′ position of nucleoside monophosphate thus rapidly regenerates phosphoric acid [28]. ATP-dependent intracellular proteolysis plays an important role in cellular physiology of bacteria [42,43]. Therefore, the increased expression of NDK promotes phosphoric acid consumption and dNTP accumulation, while the decreased expression of NT5 inhibits dephosphorylation. In bacteria, DNA recycling needs several specialized catabolic enzymes including the NT5 and NDK. The two enzymes involve in the de novo synthesis of purines in growing bacterial cells, the antibiotic DAP affects CM charges and brings about their abnormal levels to disrupt bacterial purine metabolism balance, which is at least partially responsible for DAP antibacterial activity.

Proteins interacting with NDK (Fig. 1 in Ref. [39]) and NT5 (Fig. 2 in Ref. [39]) are also tightly linked with the nucleotide acid metabolism pathway, based on a biological network analysis using an online software STRING (http://string-db.org). NDK lies in the central position to interact with several kinase proteins for nucleotide acid metabolism. For example, guanylate kinase (GMK) is an essential kinase for recycling GMP and cGMP. Adenylate kinase (ADK) is a small ubiquitous enzyme for cell growth. And thymidylate kinase (TMK) is an essential kinase for phosphorylation of dTMP to form dTDP in both de novo and salvage pathways. The other molecule NT5 is linked together with ATP-binding protein and other several uncharacterized proteins. Generally, bacterial intracellular nucleotide metabolism is achieved through coordinating with regulation of those kinase proteins. Of course, we will focus on the association of DAP with these two proteins in bacterial nucleotide acid metabolism in future study.

5. Conclusion

Our quantitative proteomic analysis revealed 51 bacterial proteins, including 34 up-regulated and 17 down-regulated, were significantly changed in response to DAP exposure at sub-inhibitory concentration. The differentially expressed bacterial proteins involve in multiple biological functions including catalytic activity, nucleotide binding, protein binding and other biological activities. On the other hand, totally 139 identified strain proteins locate in bacterial cell membrane, 7 CM proteins were significantly altered in expression level which reduced bacterial membrane potential to help DAP insertion into bacterial CM to perform antibacterial activity. Especially two important bacterial nucleotide acid metabolism associated proteins, the up-regulation of NDK and down-regulation of NT5, are validated to be a universal variation tendency against DAP treatment in several *S. aureus* strains. Furthermore, the morphological and ultrastructural alterations of DAP-treated *S. aureus* ATCC 25923 via TEM observations clearly demonstrated bacterial cell membrane was disrupted and damaged with no membrane integrity, and bacterial chromosome was aggregated, which resulted in bacterial DNA rapid release and induced bacteria death quickly. The quantitative bacterial proteomic analysis revealed DAP bactericidal targeting host proteins as a high effective antimicrobial antibiotic.

Conflict of interest

The authors declare no conflict of interest.

Significance of the study

1. Fifty-one bacterial proteome of *Staphylococcus aureus*, including 7 cell membrane proteins, were significantly alerted for responses to one antibiotic (daptomycin) treatment through an iTRAQ quantitative proteomic analysis.

2. The upregulation of NDK and downregulation of NT5 in several pathogenetic bacteria against the antibiotic treatment are a universal variation tendency.
3. This is the first time to exactly identify bacterial proteins responsible for the high effectively antimicrobial activity of this antibiotic DAP, which helps better understand its action mechanism.

Acknowledgements

This work was financially supported by the grants from National Key Basic Research Program of China (2013CB911303, 2011CB910703), the National 863 High Tech Foundation (2014AA020608), National Natural Sciences Foundation of China (31470810, 31071235), and specialized research fund for the Doctoral Program of Higher Education (20120181110025).

Appendix A. Supplementary data

Supplementary data to this article can be found online at http://dx.doi.org/10.1016/j.jprot.2016.09.014.

References

[1] S.K. Straus, R.E. Hancock, Mode of action of the new antibiotic for Gram-positive pathogens daptomycin: comparison with cationic antimicrobial peptides and lipopeptides, Biochim. Biophys. Acta 2006 (1758) 1215–1223.
[2] A. Raja, J. LaBonte, J. Lebbos, P. Kirkpatrick, Daptomycin, Nat. Rev. Drug Discov. 2 (2003) 943–944.
[3] J.M. Streit, R.N. Jones, H.S. Sader, Daptomycin activity and spectrum: a worldwide sample of 6737 clinical Gram-positive organisms, J. Antimicrob. Chemother. 53 (2004) 669–674.
[4] I.A. Critchley, D.C. Draghi, D.F. Sahm, C. Thornsberry, et al., Activity of daptomycin against susceptible and multidrug-resistant Gram-positive pathogens collected in the SECURE study (Europe) during 2000–2001, J. Antimicrob. Chemother. 51 (2003) 639–649.
[5] J.N. Steenbergen, J. Alder, G.M. Thorne, F.P. Tally, Daptomycin: a lipopeptide antibiotic for the treatment of serious Gram-positive infections, J. Antimicrob. Chemother. 55 (2005) 283–288.
[6] C.F. Carpenter, H.F. Chambers, Daptomycin: another novel agent for treating infections due to drug-resistant gram-positive pathogens, Clin. Infect. Dis. 38 (2004) 994–1000.
[7] L. Cui, E. Tominaga, H.M. Neoh, K. Hiramatsu, Correlation between reduced daptomycin susceptibility and vancomycin resistance in vancomycin-intermediate *Staphylococcus aureus*, Antimicrob. Agents Chemother. 50 (2006) 1079–1082.
[8] J.A. Silverman, N.G. Perlmutter, H.M. Shapiro, Correlation of daptomycin bactericidal activity and membrane depolarization in *Staphylococcus aureus*, Antimicrob. Agents Chemother. 47 (2003) 2538–2544.
[9] V. Laganas, J. Alder, J.A. Silverman, In vitro bactericidal activities of daptomycin against *Staphylococcus aureus* and enterococcus faecalis are not mediated by inhibition of lipoteichoic acid biosynthesis, Antimicrob. Agents Chemother. 47 (2003) 2682–2684.
[10] W.R. Scott, S.B. Baek, D. Jung, R.E. Hancock, S.K. Straus, NMR structural studies of the antibiotic lipopeptide daptomycin in DHPC micelles, BBA-Biomembranes 1768 (2007) 3116–3126.
[11] A.S. Bayer, T. Schneider, H.G. Sahl, Mechanisms of daptomycin resistance in *Staphylococcus aureus*: role of the cell membrane and cell wall, Ann. N. Y. Acad. Sci. 1277 (2013) 139–158.
[12] J.K. Muraih, A. Pearson, J. Silverman, M. Palmer, Oligomerization of daptomycin on membranes, Biochim. Biophys. Acta 2011 (1808) 1154–1160.
[13] C.T. Mascio, J.D. Alder, J.A. Silverman, Bactericidal action of daptomycin against stationary-phase and nondividing *Staphylococcus aureus* cells, Antimicrob. Agents Chemother. 51 (2007) 4255–4260.
[14] M. Junqueira, G. Domont, Microbial Proteomics, J. Proteome Res. 11 (2012) 1.
[15] M.P. Washburn, J.R. Yates III, Analysis of the microbial proteome, Curr. Opin. Microbiol. 3 (2000) 292–297.
[16] C. Graham, G. McMullan, R.L. Graham, Proteomics in the microbial sciences, Bioengineered 2 (2011) 17–30.
[17] J. Lenco, M. Link, V. Tambor, J. Zakova, et al., iTRAQ quantitative analysis of Francisella tularensis ssp. holarctica live vaccine strain and Francisella tularensis ssp. tularensis SCHU S4 response to different temperatures and stationary phases of growth, Proteomics 9 (2009) 2875–2882.
[18] W. Sianglum, P. Srimanote, W. Wonglumsom, K. Kittiniyom, S.P. Voravuthikunchai, Proteome analyses of cellular proteins in methicillin-resistant *Staphylococcus aureus* treated with rhodomyrtone, a novel antibiotic candidate, PLoS One 6 (2011), e16628.
[19] G. Pocsfalvi, G. Cacace, M. Cuccurullo, G. Serluca, et al., Proteomic analysis of exoproteins expressed by enterotoxigenic *Staphylococcus aureus* strains, Proteomics 8 (2008) 2462–2476.
[20] C. Kohler, S. Wolff, D. Albrecht, S. Fuchs, et al., Proteome analyses of *Staphylococcus aureus* in growing and non-growing cells: a physiological approach, Int. J. Med. Microbiol. 295 (2005) 547–565.
[21] X. Wu, K. Held, C. Zheng, B.J. Staudinger, J.D. Chavez, C.R. Weisbrod, J.K. Eng, P.K. Singh, C. Manoil, J.E. Bruce, Dynamic proteome response of Pseudomonas aeruginosa to tobramycin antibiotic treatment, Mol. Cell. Proteomics 14 (2015), M115.050161.
[22] A. Michalski, E. Damoc, J. Hauschild, O. Lange, A. Wieghaus, A. Makarov, N. Nagaraj, J. Cox, M. Mann, S. Horning, Mass spectrometry-based proteomics using Q Exactive, a high-performance benchtop quadrupole orbitrap mass pectrometer, Mol. Cell. Proteomics 10 (9) (2011), M111.011015.
[23] A.-C. Gingras, M. Gstaiger, B. Raught, R. Aebersold, Analysis of protein complexes using mass spectrometry, Nat. Rev. Mol. Cell Biol. 8 (2007) 645–654.
[24] H. Li, G. Li, X. Zhao, Y. Wu, W. Ma, Y. Liu, et al., Complementary serum proteomic analysis of autoimmune hepatitis in mice and patients, J. Transl. Med. 11 (2013) 146.
[25] S. Liang, Z. Xu, X. Xu, X. Zhao, C. Huang, Y. Wei, Quantitative proteomics for cancer biomarker discovery, Comb. Chem. High T Scr. 15 (2012) 221–231.
[26] C.A. Santos, A.M. Saraiva, M.A. Toledo, L.L. Beloti, et al., Initial biochemical and functional characterization of a 5′-nucleotidase from Xylella fastidiosa related to the human cytosolic 5′-nucleotidase I, Microb. Pathog. 59-60 (2013) 1–6.
[27] A.M. Chakrabarty, Nucleoside diphosphate kinase role in bacterial growth, virulence, cell signalling and polysaccharide synthesis, Mol. Microbiol. 28 (1998) 875–882.
[28] L. Robbel, M.A. Marahiel, Daptomycin, a bacterial lipopeptide synthesized by a nonribosomal machinery, J. Biol. Chem. 285 (2010) 27501–27508.
[29] S.A. Hunsucker, B.S. Mitchell, J. Spychala, The 5′-nucleotidases as regulators of nucleotide and drug metabolism, J. Pharmacol. Exp. Ther. 107 (2005) 1–30.
[30] K.L. Bogan, C. Brenner, 5′-nucleotidases and their new roles in NAD+ and phosphate metabolism, New J. Chem. 34 (2010) 845–853.
[31] S.J. Vandecasteele, W.E. Peetermans, R. Merckx, J. Van Eldere, Quantification of expression of *Staphylococcus epidermidis* housekeeping genes with Taqman quantitative PCR during in vitro growth and under different conditions, J. Bacteriol. 183 (2001) 7094–7101.
[32] M. Wu, R.E. Hancock, Interaction of the cyclic antimicrobial cationic peptide bactenecin with the outer and cytoplasmic membrane, J. Biol. Chem. 274 (1999) 29–35.
[33] W. Alborn, N. Allen, D. Preston, Daptomycin disrupts membrane potential in growing *Staphylococcus aureus*, Antimicrob. Agents Chemother. 35 (1991) 2282–2287.
[34] K.N. Miyamoto, K.M. Monteiro, C.K. da Silva, K.R. Lorenzatto, H.B. Ferreira, A. Brandelli, Comparative proteomic analysis of *Listeria monocytogenes* ATCC 7644 exposed to a sublethal concentration of nisin, J. Proteome 119 (2015) 230–237.
[35] V.G. Fowler Jr., H.W. Boucher, G.R. Corey, E. Abrutyn, A.W. Karchmer, M.E. Rupp, et al., Daptomycin versus standard therapy for bacteremia and endocarditis caused by *Staphylococcus aureus*, New. Engl. J. Med. 355 (2006) 653–665.
[36] M.H. Murthy, M.E. Olson, R.W. Wickert, P.D. Fey, Z. Jalali, Daptomycin non-susceptible meticillin-resistant *Staphylococcus aureus* USA 300 isolate, J. Med. Microbiol. 57 (2008) 1036–1038.
[37] C.I. Montero, F. Stock, P.R. Murray, Mechanisms of resistance to daptomycin in enterococcus faecium, Antimicrob. Agents Chemother. 52 (2008) 1167–1170.
[38] L. Friedman, J.D. Alder, J.A. Silverman, Genetic changes that correlate with reduced susceptibility to daptomycin in *Staphylococcus aureus*, Antimicrob. Agents Chemother. 50 (2006) 2137–2145.
[39] D. Zhang, W. Ma, G. Li, J. Liu, G. He, P. Zhang, L. Yang, H. Zhu, N. Xu, S. Liang, The interacting protein networks and nucleotide metabolism pathways related to NDK and NT5, DIB-D-16-00746.
[40] I. Lascu, P. Gonin, The catalytic mechanism of nucleoside diphosphate kinases, J. Bioenerg. Biomembr. 32 (2000) 237–246.
[41] V. Thammavongsa, J.W. Kern, D.M. Missiakas, O. Schneewind, *Staphylococcus aureus* synthesizes adenosine to escape host immune responses, J. Exp. Med. 206 (2009) 2417–2427.
[42] S. Michalik, M. Liebeke, D. Zuhlke, M. Lalk, et al., Proteolysis during long-term glucose starvation in *Staphylococcus aureus* COL, Proteomics 9 (2009) 4468–4477.
[43] D. Frees, K. Savijoki, P. Varmanen, H. Ingmer, Clp ATPases and ClpP proteolytic complexes regulate vital biological processes in low GC, gram-positive bacteria, Mol. Microbiol. 63 (2007) 1285–1295.